

Half-KFN: An Enhanced Detection Method for Subtle Covariate Drift

Bingbing Wang, Dong Xu, Yu Tang

Abstract—Detecting covariate drift is a common task of significant practical value in supervised learning. Once covariate drift occurs, the models may no longer be applicable, hence numerous studies have been devoted to the advancement of detection methods. However, current research methods are not particularly effective in handling subtle covariate drift when dealing with small proportions of drift samples. In this paper, inspired by the k -nearest neighbor (KNN) approach, a novel method called Half k -farthest neighbor (Half-KFN) is proposed in response to specific scenarios. Compared to traditional ones, Half-KFN exhibits higher power due to the inherent capability of the farthest neighbors which could better characterize the nature of drift. Furthermore, with larger sample sizes, the employment of the bootstrap for hypothesis testing is recommended. It is leveraged to calculate p -values dramatically faster than permutation tests, with speed undergoing an exponential growth as sample size increases. Numerical experiments on simulated and real data are conducted to evaluate our proposed method, and the results demonstrate that it consistently displays superior sensitivity and rapidity in covariate drift detection across various cases.

Index Terms—Bootstrap hypothesis test; Covariate drift detection; k -nearest neighbor; Permutation test.

I. INTRODUCTION

NOWADAYS, supervised learning models play a critical role in the field of machine learning, with numerous research efforts dedicated to developing a variety of application tools to drive their progress [1], [2], [3]. Typically, the assumption of supervised learning is that the training data (following distribution p) and the test data (following distribution q) are independently and identically distributed, meaning that they have the same stationary distribution, i.e., $p(X, Y) = q(X, Y)$. When this assumption does not hold, we say that dataset drift has occurred [4], [5]. Dataset drift can be classified based on whether the alteration is in covariate distribution, label distribution, or the relationship between covariates and labels [6], [7], [8]. Among them, covariate drift caused by changes in covariate distribution is one of the common and significant issues in dataset drift [9]. It refers to the situation where only when the marginal distribution of the covariate $p(X)$ deviates from $q(X)$ (i.e. $p(X) \neq q(X)$, while $p(Y|X) = q(Y|X)$). The occurrence of covariate drift may compromise the generalization ability of a trained model, increasing the risk of erroneous predictions. Therefore, covariate

drift remains a significant challenge in model deployment, and a substantial amount of research has been devoted to proposing detection methods aimed at helping to promptly identify the incidence of covariate drift [10], [11].

Goodfellow et al. [12] developed a method to generate adversarial examples by adding a specially designed small noise to the pixel values of original images, which could result in significant changes in prediction outcomes. Moreover, even if the proportion of drifting samples is subtle, they can become a fatal hidden danger that cannot be ignored for scenarios that rely heavily on models for precise predictions or critical decision-making. Such subtle covariate drift is sufficient to shake the robustness of models, seriously jeopardizing prediction accuracy and decision-making effectiveness. Nevertheless, the detection of subtle covariate drift has not been adequately emphasized. How to identify subtle covariate drift more quickly and accurately poses a challenging problem, especially in the case of large sample sizes. Thus, the motivation behind this study is based on this issue.

The contributions of this paper are as follows:

- (1) A novel, ingenious, and efficient method called Half-KFN is proposed, which demonstrates higher power compared to the traditional methods for covariate drift detection.
- (2) In scenarios with large sample sizes, the faster establishment of critical values compared to permutation tests is enabled by the use of bootstrap hypothesis testing, thereby facilitating the quicker detection of covariate drift.
- (3) Multiple comparative experiments are conducted covering different sample sizes, drift proportions, and various types of covariate drift applied to the test samples. Compared to conventional detection methods, our proposed Half-KFN combined with bootstrap hypothesis test demonstrates multifaceted superiority.

The remaining sections of this paper are organized as follows. Firstly, in Section II, we provide an overview of the latest research relevant to our study. Next, in Section III, we introduce a covariate drift detection framework based on the proposed Half-KFN statistic, employing bootstrap for expedited hypothesis testing in scenarios with large sample sizes. To demonstrate the effectiveness of our method in various scenarios, we apply this covariate drift framework to both artificial and real-world datasets in Section IV. Finally, we broadly discuss our research findings and contributions in section V. The theoretical proof in the paper is placed in the appendix.

This work was supported in part by the National Natural Science Foundation of China under Grant 12071329 and Grant 12471246. (Corresponding authors: Dong Xu.)

Bingbing Wang and Dong Xu are with the School of Mathematical Sciences, Soochow University, Suzhou 215031, China (e-mail: bbwang-stat1@stu.suda.edu.cn; xd0309@suda.edu.cn).

Yu Tang is with the School of Future Science and Engineering, Soochow University, Suzhou 215006, China (e-mail: ytang@suda.edu.cn).

II. RELATED WORK

A. Covariate drift detection

Covariate drift detection methods are typically categorized based on different sample formats, which can be classified into streaming/online mode [13], [14] and two-sample tests in a batch/offline mode [15], [16]. To address the first mode, Xu et al. [17] propose using multiple signals to capture a wide range of characteristics of the data. In addition, Polo et al. [18] demonstrated the importance of dimensionality reduction or feature selection for model generalization in the context of covariate shift adaptation. Certain methods assist in identifying issues such as model performance degradation caused by changes in data distribution, promptly triggering alerts [19], [20]. Some methods specifically focus on the covariate drift correction to improve the robustness and generalization ability of the model [21], [22], [23]. To address the second mode, Rabanser et al. [15] conducted a comparative study on various dimensionality reduction methods using traditional two-sample tests in the context of covariance shift detection. By enhancing the detection framework, Castle et al. [24] represented the data as model explanations in the form of gradient times input, providing additional information about the data domain for two-sample tests, which helps improve the sensitivity of drift detection.

B. A dimension reduction method

In the current context of supervised learning, input data is commonly characterized by high dimensionality, which presents challenges. To address the detection of covariate drift in high-dimensional input data, Lipton et al. [25] proposed a method called black box drift detection (BBSD) which is related to detect covariate drift [15], concept drift [26], label drift [27] and more general forms of nonstationarity. Furthermore, Rabanser et al. [15] propose using the softmax outputs (BBSDs) of a label classifier, trained on source data, as a dimension-reduced representation. They also found that compared to various dimensionality reduction methods such as principal components analysis (PCA), sparse random projection (SRP), untrained autoencoders (UAE), and trained autoencoders (TAE), using BBSDs can achieve the best performance. It simply requires the utilization of an arbitrary soft-classifier f (required that the confusion matrix constructed from the classification results on the training data is invertible) to detect drift in the distributions of each class after dimensionality reduction of the covariates, i.e., $p(f(X)) \neq q(f(X))$.

C. Two-sample test

Once the dimensionality reduction method has been determined, it is natural to proceed with the detection method. The multivariate two-sample test has been extensively investigated in studies, with notable contributions from research papers that have explored methods such as the Maximum Mean Discrepancy (MMD) test [28], [29], [30], Friedman-Rafsky (FR) test [31], [32], and energy test [33], [34]. Moreover, KNN test proposed by Schilling [35] and Henze [36] is a famous non-parametric method for multivariate two-sample

test. Djolonga and Krause [37] devised differentiable adaptations of the KNN test, thereby establishing the asymptotic normality under specific conditions. By smoothing classical KNN statistic, the computation of smooth p -values becomes feasible under permutation distribution. Although KNN test has the asymptotic normality under large samples [36], [38], [35], [39], the detection effect is not satisfactory in special scenarios with small proportion drifting samples. For this reason, current methods for detecting covariate drift still have limitations, which highlight the crucial necessity for research aimed at accurately identifying subtle covariate drift.

D. Resampling hypothesis test

In the statistical inference task of a two-sample test, resampling methods are flexible and powerful tools, which involve making repeated random samples from a dataset for statistical inference [40], [41]. Resampling hypothesis test, which includes permutation test and bootstrap hypothesis test, is utilized to estimate the distribution of statistics, calculate confidence intervals, assist in assessing the robustness of parameter estimates, and more. These techniques demonstrate significant potential and impact in practical applications.

When the population distribution is unclear, one method for statistical inference is permutation test [42], [43], [5]. One of the most significant advantages of using permutation methods for inference is their robustness [44]. Permutation tests have relatively weak assumptions about the statistical data, making them more robust than corresponding parametric methods when dealing with outliers or extreme distributions. Permutation tests are particularly effective in tests with small sample sizes [45], [46]. However, a potential issue arises as the sample size increases, leading to longer testing times [47]. Another detection method involves obtaining critical values through bootstrap under the null hypothesis [48], [49], where the Central Limit Theorem ensures the asymptotic normality of the mean of the test statistic in large sample scenarios. If the sample size is sufficiently large, even if the distribution of the original data is non-normal, parametric tests can still be employed [50], [51].

III. METHODOLOGY

Our approach highlights two notable innovations. Firstly, after dimensionality reduction through BBSDs, we craft the Half-KFN statistic using Euclidean distance. Based on the characteristics of farthest neighbors, this statistic can more precisely represent the magnitude of differences arising from small proportions of covariate drifting samples. Secondly, we observe significant computation time and resource consumption issues when performing permutation testing to calculate p -values in statistical inference involving larger sample sizes. So, we propose employing bootstrap to construct a new statistic defined as the mean of Half-KFN, and we calculate its expectation and asymptotic variance for statistical inference.

Experimental results demonstrate that our method exhibits advantages in various aspects. It is not only capable of conducting statistical inference more rapidly and accurately, but also consumes less computational resources. Furthermore, it effectively controls the probability of Type-I error.

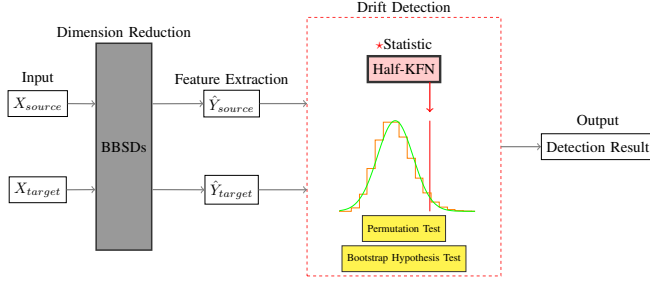


Fig. 1. Data drift detection architecture with Half-KFN. First, data are respectively sampled from source and target distributions. Subsequently, the BBSDs method is applied for performing dimensionality reduction. Then, our proposed statistical measure, Half-KFN, is utilized to quantify the magnitude of drift differences. Finally, permutation test and bootstrap hypothesis test is employed to obtain the corresponding p -value.

A. Problem setup

Let $\{X_1, \dots, X_{n_1}\}$ and $\{X'_1, \dots, X'_{n_2}\}$ be two datasets of covariates from the source distribution p and the target distribution q in \mathbb{R}^C , respectively. We make the assumption of independent and identically distributed (i.i.d.) observations within each dataset, and further assume that the datasets are mutually independent.

The problem of covariate drift detection here is to test the hypothesis $H_0 : p(X) = q(X)$ against the completely general alternative $H_1 : p(X) \neq q(X)$. In the context of subtle covariate shift detection, our primary concerns encompass two core questions: (1) How to sensitively capture the drifted samples? (2) How to perform the detection faster with larger sample sizes?

B. Dimension Reduction

High-dimensional covariate input data usually requires efficient dimensionality reduction techniques to simplify data representation and extract key information. It is worth noting that without making assumptions about the data, these mappings, which reduce the dimensionality from C to L (with $C > L$), are typically surjective, meaning each output element has at least one corresponding input, and multiple inputs can map to the same output. Although it is possible to construct special cases where the input distribution changes while the low-dimensional latent representation distribution remains unchanged, such situations are likely very rare in practical non-adversarial environments. Hence, dimensionality reduction techniques are practical and can effectively simplify high-dimensional data and extract key information.

Lipton et al. [25] proposed a method called Black Box drift Detection (BBSDs), demonstrating that if one has an arbitrary pre-trained label classifier f , and its confusion matrix on the source distribution data is invertible, detecting whether covariate drift has occurred is equivalent to detecting whether $p(f(X))$ equals $q(f(X))$. It states that for any fixed mea-

asurable function $f : \mathbb{R}^C \rightarrow \mathbb{R}^L$ and for every measurable $S \subset \mathbb{R}^L$,

$$p(f(X)) = q(f(X)) \Rightarrow p(X \in f^{-1}(S)) = q(X \in f^{-1}(S)). \quad (\text{III.1})$$

Rabanser et al. [15] explored a series of dimensionality reduction techniques and conducted comparative experiments under various simulated covariate drift scenarios. The experiments showed that BBSDs performed best in dimensionality reduction across various drift simulations. Therefore, in this paper, we will use the BBSDs method for dimensionality reduction.

Assume there is a label classifier f whose confusion matrix is invertible and is a mapping from \mathbb{R}^C to \mathbb{R}^L . Let the BBSDs dimensionality reduction result be $\hat{Y} = f(X)$, and \hat{Y} represents the softmax vector output $(\hat{y}_1, \hat{y}_2, \dots, \hat{y}_L)$. Let $n = n_1 + n_2$, $\omega_1 = \{1, \dots, n_1\}$, $\omega_2 = \{n_1 + 1, \dots, n\}$. Define $D^{(1)} = \{\hat{Y}_i\}_{i=1}^{n_1}$, $D^{(2)} = \{\hat{Y}_i\}_{i=n_1+1}^n$, and denote the combined sample set as $D = \{\hat{Y}_i\}_{i=1}^n$, where

$$\hat{Y}_i = \begin{cases} f(X_i), & i \in \omega_1, \\ f(X'_{i-n_1}), & i \in \omega_2. \end{cases} \quad (\text{III.2})$$

C. Statistic of Half k -farthest neighbor (Half-KFN)

Our statistic represents an improvement upon the KNN statistic [39]. In the context of previous detection scenarios, KNN test plays a pivotal role, being not only conceptually straightforward but also possessing an analytically tractable null distribution. Consequently, with a sufficiently large sample size, the utilization of its simple and precise null distribution allows for intuitive detection, showcasing its inherent efficiency advantage.

However, to achieve a more sensitive detection for subtle covariate drift, enhancements to the KNN statistic are imperative. Naturally, for a small subset of drifted samples, their predictive accuracy is evidently diminished after undergoing BBSDs dimensionality reduction, compared to the normal samples unaffected by drift. In other words, when drifted samples are processed through an arbitrary label classifier f for classification, resulting in a vector-form classification outcome, their predictive performance is highly likely to deteriorate significantly compared to the classification results of normal samples not subject to drift. In order to capture these deteriorated samples effectively, we have devised a novel statistic to detect instances where the predictive performance degrades due to drift.

In this paper, we employ the notation $\|\cdot\|$ to signify the L_2 norm, and define the k -th intra-class farthest neighbor of \hat{Y}_i to be $\hat{Y}_{j'}$, satisfying $\|\hat{Y}_{j'} - \hat{Y}_i\| > \|\hat{Y}_j - \hat{Y}_i\|$ for exactly $k - 1$ indices j' ($1 \leq j' \leq n, j' \neq i, j$), and ensuring that the indices of the maximum elements in \hat{Y}_i and $\hat{Y}_{j'}$ are the same, which means \hat{Y}_i and $\hat{Y}_{j'}$ are in the same class. In simpler terms, the intra-class k farthest neighbors of \hat{Y}_i refer to the k samples of the same class as \hat{Y}_i that are farthest away from \hat{Y}_i . We define two events: $A_{i,j}^{(k)} \triangleq \{\hat{Y}_j \text{ is one of the intra-class } k \text{ farthest neighbors of } \hat{Y}_i\}$ and $B_{i,j} \triangleq \{\hat{Y}_i \text{ is from } p \text{ and } \hat{Y}_j \text{ is from } q\}$.

In scenarios with sufficiently large sample sizes, we can establish the distribution function or an approximate distribution for the T_{k,n_1} statistic. By leveraging known properties of probability distributions, we can make statistical inferences. This method helps avoid the need for extensive permutations, thereby saving time and computational resources.

D. Permutation Test

Once we possess a statistical measure capable of quantifying the extent of covariate drift, we can utilize hypothesis testing to formally examine the null hypothesis. It is crucial to recognize that Y is a continuous probability vector, as this is an essential requirement for the algorithm to function properly.

Consider conducting a permutation test with P permutations. In each permutation $t \in \{1, \dots, P\}$, we define the two datasets, denoted as $D^{(1,t)} = \{\hat{Y}_i^{(t)}\}_{i=1}^{n_1}$ and $D^{(2,t)} = \{\hat{Y}_i^{(t)}\}_{i=n_1+1}^n$, which are randomly split by D . It is necessary to ensure that the sample sizes of the two sets are consistent with the sizes of $D^{(1)}$ and $D^{(2)}$, respectively.

Moreover, to guarantee the absence of repeated values within the set $\{T_{k,n_1}^{(t)}\}_{t=1}^P$, we add minor Gaussian noise perturbations centered around zero with a variance of σ_{noise}^2 , to T_{k,n_1} and $T_{k,n_1}^{(t)}$, for each permutation. That is

$$T = T_{k,n_1} + N(0, \sigma_{noise}^2), \quad (\text{III.6})$$

$$T^{(t)} = T_{k,n_1}^{(t)} + N(0, \sigma_{noise}^2). \quad (\text{III.7})$$

Then, we evaluate each hypothesis of interest by calculating a p -value in the following form:

$$p = \frac{\sum_{t=1}^P (I(T \leq T^{(t)}))}{P}. \quad (\text{III.8})$$

We fix a predetermined significance level $\alpha \in (0, 1)$. After calculating the particular p -value pertaining to a given null hypothesis, reject it if $p \leq \alpha$.

Proposition 1. For every $\alpha \in (0, 1)$, under H_0 ,

$$\mathbb{P}(p \leq \alpha) \leq \alpha. \quad (\text{III.9})$$

The above proposition 1 serves as evidence to support the validity of such tests in controlling the Type-I error rate. By doing so, these tests effectively manage and minimize false alarms, ensuring accurate and reliable results. The proof (see Appendix A) employed the theory of permutation tests (refer to Lehmann et al. [52] for details).

E. Bootstrap Hypothesis Test

In the case of a sufficiently large sample size, we can compute the expectation and variance of the T_{k,n_1} statistic. Although the exact distribution of T_{k,n_1} may be unknown, the Central Limit Theorem informs us that the distribution of the means of T_{k,n_1} approximates a normal distribution when the sample size is sufficiently large. By computing its expectation and variance, we can utilize the properties of the

Algorithm 2 Permutation Test of Half-KFN

Input: Samples $\{X_1, \dots, X_{n_1}\}$ from source distribution; samples $\{X'_1, \dots, X'_{n_2}\}$ from target distribution; a trained soft-classifier $f: \mathbb{R}^C \rightarrow \mathbb{R}^L$; the number of farthest neighbors k ; significance level α ; the variance of Gaussian noise σ_{noise}^2 .

Output: decision (drift or no-drift?)

- 1: Compute Half-KFN statistic T_{k,n_1} through Algorithm 1
 - 2: Add Gaussian noise: $T = T_{k,n_1} + N(0, \sigma_{noise}^2)$
 - 3: **for** $t = 1$ to P **do**
 - 4: $(D^{(1,t)}, D^{(2,t)}) = \left(\left\{ \hat{Y}_i^{(t)} \right\}_{i=1}^{n_1}, \left\{ \hat{Y}_i^{(t)} \right\}_{i=n_1+1}^n \right) \leftarrow \text{random split of } \left\{ \hat{Y}_i \right\}_{i=1}^n$
 - 5: Execute step 3 to step 20 of Algorithm 1 and compute statistic of Half-KFN $_t$: $T_{k,n_1}^{(t)}$
 - 6: Add Gaussian noises: $T^{(t)} = T_{k,n_1}^{(t)} + N(0, \sigma_{noise}^2)$
 - 7: **end for**
 - 8: **if** $\frac{\sum_{t=1}^P (I(T \leq T^{(t)}))}{P} < \alpha$ **then**
 - 9: decision \leftarrow drift
 - 10: **else**
 - 11: decision \leftarrow no-drift
 - 12: **end if**
 - 13: **return** decision
-

normal distribution for statistical inference, thereby facilitating the detection task in the context of large sample sizes.

To perform the large sample distribution test based on T_{k,n_1} , bootstrap is performed in populations p and q for a specific number of resampling operations (assumed to be M times), ensuring that the sample size remains constant for each resampling operation. This process generates M sets of random samples, and each set of samples undergoes the aforementioned calculations to obtain the statistic $T_{k,n_1,m}$, where $m = 1, \dots, M$. Subsequently, the average of these M statistics, $\overline{T_{k,n_1}} = \frac{\sum_{m=1}^M T_{k,n_1,m}}{M}$, corresponding to the M sets of samples, is computed.

Theorem III.1. Let $FN_i(r)$ represent the r -th intra-class farthest neighbor of \hat{Y}_i . Define that

$$I_i(r) = \begin{cases} 1, & FN_i(r) \text{ and } \hat{Y}_i \text{ belong to different sample sets,} \\ 0, & \text{otherwise.} \end{cases} \quad (\text{III.10})$$

The Half-KFN statistic considered when testing H_0 are represented as follows:

$$T_{k,n_1} = \frac{1}{n_1 k} \sum_{i=1}^{n_1} \sum_{r=1}^k I_i(r). \quad (\text{III.11})$$

An alternative articulation of the Half-KFN statistic shown by Equation III.11 is synonymous with Equation III.5. The proof of Theorem III.1 is given in the Appendix B.

Assume that as n_1 and n_2 approach infinity, we have $\lim_{n \rightarrow \infty} \frac{n_i}{n} = \lambda_i$, where $i = 1, 2$. In this context, we can consider the following two probabilities:

- (1) $p_1(r, s) = P_{H_0}(FN_i(r) = \hat{Y}_j, FN_j(s) = \hat{Y}_i)$,
- (2) $p_2(r, s) = P_{H_0}(FN_i(r) = FN_j(s))$.

For any given \hat{Y}_i and \hat{Y}_j , with s and r specified, $p_1(r, s)$ and $p_2(r, s)$ respectively represent the probabilities that they are mutually farthest neighbors and share a farthest neighbor.

Note that if the sample size n is large, rather than tests based on the permutation principle, one can utilize tests based on the asymptotic null distributions of $\overline{T_{k,n_1}}$, as outlined in the following theorem.

Theorem III.2. *If n grows to infinity in such a way that $n_1/n \rightarrow \lambda_1, n_2/n \rightarrow \lambda_2$ for $\lambda_1, \lambda_2 \in (0, 1)$, then for any fixed dimension d and any fixed k , $\frac{\overline{T_{k,n_1} - \mu}}{\sqrt{\sigma^2/M}}$ asymptotically follows a standard normal distribution under H_0 , where*

$$\mu = \lim_{n \rightarrow \infty} E_{H_0}(T_{k,n_1,m}) = \lim_{n \rightarrow \infty} \frac{n_2}{n-1} = \lambda_2, \quad (\text{III.12})$$

$$\begin{aligned} \sigma^2 &= \lim_{n \rightarrow \infty} \text{Var}_{H_0}(T_{k,n_1,m}) \\ &= \lambda_2^2 \frac{\sum_{r=1}^k \sum_{s=1}^k p_1(r,s)}{k^2} + \lambda_1 \lambda_2 \frac{\sum_{r=1}^k \sum_{s=1}^k p_2(r,s)}{k^2} \end{aligned} \quad (\text{III.13})$$

The proof of Theorem III.2 is given in the Appendix C.

Algorithm 3 Bootstrap Hypothesis Test of Half-KFN

Input: Source dataset X_{source} ; target dataset X_{target} ; the number of resampling operation M ; a trained soft-classifier $f: \mathbb{R}^C \rightarrow \mathbb{R}^L$; the number of farthest neighbors k ; significance level α ; $U \sim N(0, 1)$; probability of mutually farthest neighbors $p_1(r, s)$; probability of share a farthest neighbor $p_2(r, s)$.

Output: decision (drift or no-drift?)

- 1: Resample n_1 and n_2 samples from the source and target datasets respectively, for M times:
 - 2: $\lambda_1 \leftarrow \frac{n_1}{n}, \lambda_2 \leftarrow \frac{n_2}{n}$
 - 3: **for** $m = 1$ to M **do**
 - 4: $\{X_{1,m}, \dots, X_{n_1,m}\} \leftarrow$ random resample from X_{source}
 - 5: $\{X'_{1,m}, \dots, X'_{n_2,m}\} \leftarrow$ random resample from X_{target}
 - 6: Execute Algorithm 1 and compute Half-KFN $_m: T_{k,n_1,m}$
 - 7: **end for**
 - 8: $\overline{T_{k,n_1}} \leftarrow \frac{\sum_{m=1}^M T_{k,n_1,m}}{M}$
 - 9: $\mu \leftarrow \lambda_2$
 - 10: $\sigma^2 \leftarrow \lambda_2^2 \frac{\sum_{r=1}^k \sum_{s=1}^k p_1(r,s)}{k^2} + \lambda_1 \lambda_2 \frac{\sum_{r=1}^k \sum_{s=1}^k p_2(r,s)}{k^2}$
 - 11: **if** $P(U > \left| \frac{\overline{T_{k,n_1}} - \mu}{\sqrt{\sigma^2/M}} \right|) < \alpha/2$ **then**
 - 12: decision \leftarrow drift
 - 13: **else**
 - 14: decision \leftarrow no-drift
 - 15: **end if**
 - 16: **return** decision
-

The subsequent task involves estimating $p_1(r, s)$ and $p_2(r, s)$. However, as L and k grow larger, the computational complexity associated with these estimates escalates significantly. To mitigate this complexity, we focus on the one-dimensional maximum probability value, denoted as $\max(\hat{Y}_i)$, within each vector $\hat{Y}_i = (\hat{y}_{i1}, \hat{y}_{i2}, \dots, \hat{y}_{iL})$ for $i \in \{1, \dots, n\}$. Additionally, it is noted that in Section III-B, dimensionality reduction is performed on the feature data by generating a softmax vector output using a label classifier f . In this vector, each dimension represents the probability value for each class, with the dimension having the highest probability value typically considered as the class to which the sample belongs. This dimension is notably representative and holds significant importance in drift detection. Consequently, we will consider drift detection based on the dimension with the highest probability value.

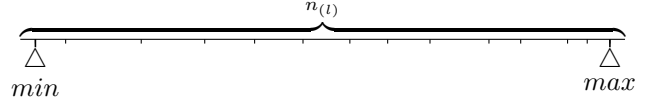


Fig. 2. When considering the dimension $\max(\hat{Y}_i)$ with $k = 1$, there exists only one pair of samples that are mutual farthest neighbors, distinctly marked by triangles.

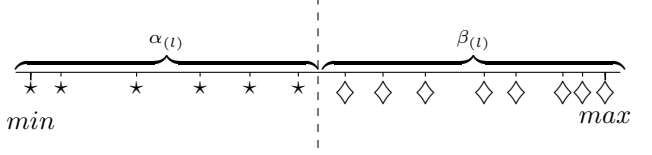


Fig. 3. When considering the dimension $\max(\hat{Y}_i)$ with $k = 1$, pairs of samples located on the same side of the dashed line ($\frac{\min + \max}{2}$) share a farthest neighbor.

For example, we consider the simplest case when $k = 1$. As k increases, $p_1(r, s)$ and $p_2(r, s)$ are estimated using the same principles and framework as described below, but the complexity of the situation and computations grows, leading to increased time costs.

Notice that we consider the intra-class situation, for each class $l \in \{1, \dots, L\}$, there are $n_{(1,l)}$ samples from q and $n_{(2,l)}$ samples from p , resulting in a total of $n_{(l)}$ samples. Since the Half-KFN statistics of each class are independent, then $\text{Var}_{H_0}(T_{k,n_1,m}) = \sum_{l=1}^L \text{Var}_{H_0}(T_{k,n_{(1,l)},m}) \cdot \frac{n_{(1,l)}^2}{n_1^2}$. The maximum and minimum values among these $n_{(l)}$ samples are recorded as shown in Figs. 2 and 3 below.

From Fig. 2, it can be observed that there is only one pair of samples that are mutually farthest neighbors (marked by triangles). Meanwhile, pairs of samples sharing a farthest neighbor can only be simultaneously distributed on one side of the dashed line in Fig. 3. In other words, pairs of samples distributed on the left side of the dashed line (marked by stars) share a farthest neighbor, i.e, the minimum point, while pairs of samples distributed on the right side of the dashed line (marked by diamonds) also share a farthest neighbor, i.e, the maximum point.

$$p_1(1, 1) = \lim_{n \rightarrow \infty} \sum_{l=1}^L \frac{1}{\binom{n_{(l)}}{2}} \cdot \frac{n_{(1,l)}^2}{n_1^2}, \quad (\text{III.14})$$

$$p_2(1, 1) = \lim_{n \rightarrow \infty} \sum_{l=1}^L \frac{\binom{\alpha_{(l)}}{2} + \binom{\beta_{(l)}}{2}}{\binom{n_{(l)}}{2}} \cdot \frac{n_{(1,l)}^2}{n_1^2}. \quad (\text{III.15})$$

We can keep track of the number of points falling to the left of the dashed line as $\alpha_{(l)}$ and the number falling to the right as $\alpha_{(2,l)}$ among $n_{(l)}$ samples, where $\sum_{l=1}^L (\alpha_{(l)} + \beta_{(l)}) = n$. This way, we can estimate $p_1(1, 1)$ and $p_2(1, 1)$ based on this information as shown in the formula III.14 and III.15.

Hence, the asymptotic variance can be simplified into a more straightforward form. Experimental evidence suggests that this method of statistical inference is more quickly in larger sample sizes, and exhibits higher power when testing for subtle drift compared to other detection methods.

IV. EXPERIMENTAL EVALUATION

Experiments in this section utilize PyTorch’s built-in distribution package. To run the experiments, we used a machine running a 64-bit operational system with 16 GB of RAM and a 3.20 GHz AMD Ryzen 7 5800H with Radeon Graphics CPU. The source code of Half-KFN is available online¹.

A. Experiments on Simulated Data

The simulation datasets consist of training set $\{(X_i, Y_i)\}_{i=1}^{6000}$ and test set $\{(X'_j)\}_{j=1}^{3000}$. For training set, there are a total of 3 categories, each of which contains 2000 samples, which means

$$X_i \sim \begin{cases} U_5(1, 2), & 1 \leq i \leq 2000, \\ U_5(5, 6), & 2001 \leq i \leq 4000, \\ U_5(10, 11), & 4001 \leq i \leq 6000, \end{cases}$$

$$Y_i = \begin{cases} 1, & 1 \leq i \leq 2000, \\ 2, & 2001 \leq i \leq 4000, \\ 3, & 4001 \leq i \leq 6000. \end{cases}$$

The test set consists of 3000 unlabeled samples, initially maintaining a covariate distribution consistent with the training set when no simulated drift is introduced. In the experiment, a softmax regression multiclassifier is employed as BBSDs for simplicity. During the model training process, the cross-entropy loss function is employed, and the model parameters are iteratively optimized using gradient descent. The loss function is shown in Fig. 4.

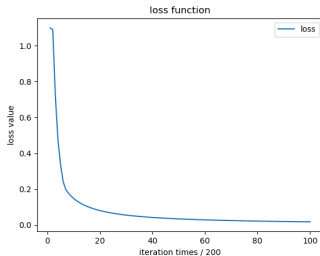


Fig. 4. The graphical representation of the loss variation during the training process of a linear classifier is obtained. The classifier parameters are estimated using gradient descent optimization. A total of 2×10^4 iterations are performed, and the loss value is recorded every 250 iterations. These recorded values are then utilized to generate a loss variation graph, enabling visualization of the optimization progress throughout the training process.

One sample set serves as the control dataset without any modifications (analogous to the source distribution), while the other sample set serves as the simulated drift dataset (analogous to the target distribution), where a proportion of δ samples are subjected to the addition of Gaussian noise with a variance of σ_{gn} . The experiments are conducted with sample sizes of $n_1 = n_2 \in \{100, 200, 500, 1000\}$. The simulated drift involves adding Gaussian noise with a standard deviation of $\sigma_{gn} = 20$ to a subset of samples in the testing set, with a proportion of $\delta \in \{0, 0.01, 0.05\}$. From the results in Table

I, it is evident that Half-KFN exhibits the best performance among the methods evaluated.

TABLE I
EVALUATION RESULTS OF OF DIFFERENT ALGORITHMS. THE RESULTS INCLUDE THE TYPE-I ERROR (WHEN $\delta = 0$) AND POWER (WHEN $\delta \in \{0.01, 0.05\}$) WITH GAUSSIAN NOISE TO A SUBSET OF SAMPLES IN THE TESTING SET.

δ	n_1	MMD	Energy	FR	KNN	Ours ¹	Ours ²
0	100	0.05	0.08	0.06	0.09	0.03	0.04
	200	0.03	0.05	0.03	0.04	0.01	0.05
	500	0.01	0.03	0.02	0.04	0.03	0.01
	1000	0.01	0.06	0.01	0.05	0.03	0.05
0.01	100	0.05	0.05	0.06	0.02	0.12	0.30
	200	0.08	0.09	0.06	0.03	0.13	0.70
	500	0.05	0.07	0.04	0.09	0.37	1.00
	1000	0.04	0.08	0.05	0.05	0.65	1.00
0.05	100	0.07	0.08	0.06	0.07	0.41	1.00
	200	0.07	0.07	0.07	0.14	0.72	1.00
	500	0.07	0.19	0.06	0.11	0.99	1.00
	1000	0.08	0.23	0.09	0.19	1.00	1.00

¹ Half-KFN with permutation test

² Half-KFN with bootstrap hypothesis test

TABLE II
EVALUATION RUNTIME RESULTS OF DIFFERENT ALGORITHMS FOR A SINGLE RUN.

n_1	MMD	Energy	FR	KNN	Ours ¹	Ours ²
100	0.23	0.22	0.19	0.19	0.16	0.04
200	0.50	0.52	0.47	0.48	0.44	0.08
500	3.03	3.14	3.01	3.05	2.19	0.31
1000	13.10	13.79	13.08	13.31	8.73	1.14

¹ Half-KFN with permutation test

² Half-KFN with bootstrap hypothesis test

In addition, we recorded the runtime of the above methods in a single run, as shown in the Table II. It can be seen that with the increase in sample size, the proposed bootstrap hypothesis test of Half-KFN not only demonstrates a higher advantage in detecting power, but also has the fastest detection rate.

B. Experiments on Real Data

This section outlines the experimental framework used to evaluate the proposed approach on real data. It details the datasets, specific configurations and evaluation metrics utilized to rigorously test the approach and demonstrate its effectiveness in practical scenarios.

1) *Datasets*: We analyze two benchmark datasets, MNIST, Fashion-MNIST and CIFAR-10, to further evaluate the proposed methodology.

MNIST ($N_{tr} = 5 \times 10^4$; $N_{val} = 1 \times 10^4$; $N_{te} = 1 \times 10^4$; $D = 28 \times 28 \times 1$; $C = 10$ classes) is a handwritten digit dataset consisting of 10 categories such as ‘0’, ‘1’, ‘2’, ‘3’, ‘4’, ‘5’, ‘6’, ‘7’, ‘8’, and ‘9’.

Fashion-MNIST ($N_{tr} = 5 \times 10^4$; $N_{val} = 1 \times 10^4$; $N_{te} = 1 \times 10^4$; $D = 28 \times 28 \times 1$; $C = 10$ classes) is a fashion product grayscale images dataset of clothing items, such as T-shirt/top, trouser, pullover, dress, coat, sandals, shirt, sneaker, bag and ankle boots. It consists of 10 categories, each containing 6×10^3 training images and 1×10^3 testing images.

¹<https://github.com/bbwang1030/Half-KFN>

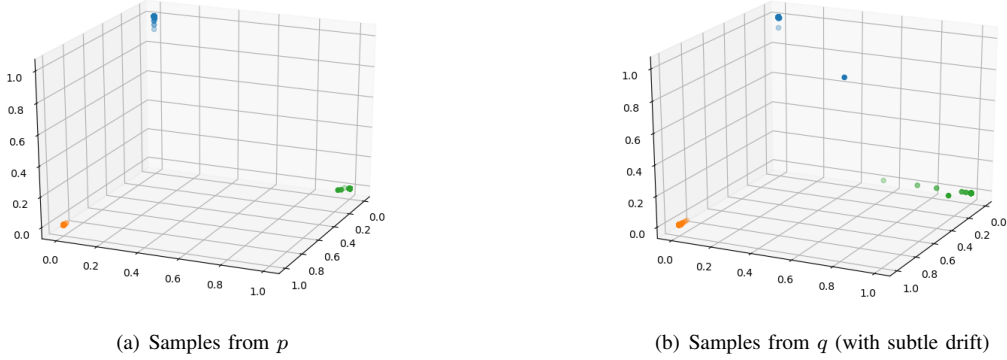


Fig. 5. The visualization of the source distribution (p) and target distribution (q) of MNIST dataset after dimensionality reduction by BBSDs (which is actually 10-dimensional data, but only three dimensions are shown for visualization purposes).

CIFAR-10 ($N_{tr} = 4 \times 10^4$; $N_{val} = 1 \times 10^4$; $N_{te} = 1 \times 10^4$; $D = 32 \times 32 \times 3$; $C = 10$ classes) is a natural image dataset composed of 10 categories, such as airplane, automobile, bird, cat, deer, dog, frog, horse, ship and truck. Each category consists of 5×10^3 samples in the training set and 1×10^3 samples in the testing set.

2) *Dimensionality reduction mode*: Subsequently, we employ a trained ResNet-18 as the classifier, a deep neural network with residual structure. The model employs stochastic gradient descent with momentum, processing 128 samples per batch for 200 epochs, with early stopping. The input consists of image samples from the source distribution and the target distribution. The output is the class probability vector obtained from the model for each image sample, derived through the softmax function. Fig. 5 presents a visual example of dimensionality reduction using BBSDs on MNIST.

3) *Experimental parameter settings*: The experimental simulation of each drift detection involves the process of substituting a certain proportion (denoted by $\delta \in \{0, 0.01, 0.05, 0.1\}$) of samples in the test set with drift samples. Each subplot represents the trend of Type-I error ($\delta = 0$) or detection power ($\delta \in \{0.01, 0.05, 0.1\}$) with sample sizes of $n_1 = n_2 \in \{100, 200, 500, 1000\}$. In this section, we set the significant level of $\alpha = 0.05$. Furthermore, we set $k = 1$ in tests of KNN, SmoothKNN and Half-KFN. However, when performing bootstrap hypothesis tests, utilizing larger values of k may yield benefits, albeit at the expense of a longer testing duration. Similarly, irrespective of the chosen value of M , our method will offer best power and maintain control the Type-I error. Nevertheless, opting for larger M values will inevitably result in a longer testing time. Therefore, in these experiments we adopt $M = 10$ for our bootstrap hypothesis tests. Undoubtedly, swiftly and accurately identifying drift anomalies and triggering alerts are crucial in data drift detection.

4) *Drift types*: Various types of drift occur, with the simulation incorporating adversarial drift, Gaussian noise drift, and image drift.

Adversarial drift (adv) is characterized by the substitution of a subset of samples within the test set with adversarial samples. It aims to introduce intentionally crafted inputs. Rauber et al. [53] [54] launched a toolbox called Foolbox, which

provides a vast array of methods for generating adversarial examples.

Gaussian noise drift (gn) involves the introduction of random noise, originating from a Gaussian distribution, to a specific subset of image pixels within the test set. The purpose of this manipulation is to simulate real-world scenarios where images might exhibit noise.

Image drift (img) refers to the systematic augmentation of a subset of images within the test set, employing an image generator. This augmentation process comprises various transformations including rotation, horizontal and vertical translation, perspective transformation, as well as random scaling within predefined bounds. By applying this drift, the objective is to expand the diversity of encountered images during testing, which is generally related to the model’s generalization ability.

5) *Execution performance*: The average p -value is shown in Table III and IV, and their standard deviation. The results indicate that, without drift, the average p -value of our test is approximately 0.5. However, in the presence of subtle drift, the average p -value of our test decreases, accompanied by a smaller standard deviation.

We conduct comparative experiments between Half-KFN and traditional techniques, including MMD, Energy, FR, KNN, and SmoothKNN, to compare their Type-I error and power. The experimental results of these distinct drift types are depicted in Figs. 6, 7 and 8, respectively. Particularly, our bootstrap hypothesis test (red line) exhibits significant advantages in terms of test performance for subtle drift. The effectiveness of the permutation test (blue line) follows.

6) *Execution time*: Furthermore, we compared the inference time of the permutation test with the bootstrap hypothesis test in Fig. 9, especially in large sample scenarios. With the gradual increase in sample size, our proposed bootstrap hypothesis test of Half-KFN demonstrates significantly shorter inference time per single run compared to the permutation test when detecting drift. This method not only exhibits higher detection power but also showcases faster detection speed, presenting a considerable advantage from various perspectives.

TABLE III
 DRIFT DETECTION RESULTS WITH REAL-WORLD DATASETS, MEAN OF p -VALUE AND STANDARD DEVIATION UNDER H_0 ($\delta = 0$). SEVEN ALGORITHMS ARE RUN 100 TIMES ON SOURCE AND TARGET SETS OF 500 SAMPLES EACH, GENERATED WITH DIFFERENT RANDOM SEEDS.

dataset	shift type	MMD	Energy	FR	KNN	SmoothKNN	Ours ¹	Ours ²
MNIST	adv	0.45 ± 0.28	0.49 ± 0.30	0.45 ± 0.28	0.49 ± 0.28	0.48 ± 0.28	0.41 ± 0.28	0.44 ± 0.27
	gn	0.50 ± 0.29	0.48 ± 0.30	0.50 ± 0.29	0.45 ± 0.29	0.44 ± 0.29	0.47 ± 0.29	0.52 ± 0.31
	img	0.50 ± 0.29	0.48 ± 0.30	0.50 ± 0.29	0.45 ± 0.29	0.44 ± 0.29	0.46 ± 0.29	0.52 ± 0.31
Fashion-MNIST	adv	0.50 ± 0.31	0.51 ± 0.31	0.50 ± 0.31	0.51 ± 0.30	0.51 ± 0.30	0.50 ± 0.28	0.46 ± 0.29
	gn	0.51 ± 0.30	0.51 ± 0.31	0.51 ± 0.29	0.53 ± 0.30	0.52 ± 0.30	0.51 ± 0.29	0.49 ± 0.28
	img	0.51 ± 0.30	0.51 ± 0.31	0.51 ± 0.29	0.53 ± 0.30	0.52 ± 0.30	0.51 ± 0.29	0.49 ± 0.28
CIFAR10	adv	0.55 ± 0.27	0.53 ± 0.30	0.56 ± 0.27	0.54 ± 0.30	0.54 ± 0.30	0.54 ± 0.30	0.48 ± 0.29
	gn	0.56 ± 0.27	0.51 ± 0.30	0.56 ± 0.27	0.53 ± 0.31	0.52 ± 0.31	0.53 ± 0.30	0.51 ± 0.30
	img	0.56 ± 0.27	0.51 ± 0.30	0.56 ± 0.27	0.53 ± 0.31	0.52 ± 0.31	0.53 ± 0.30	0.51 ± 0.30
Avg		0.52	0.50	0.52	0.51	0.50	0.50	0.49

¹ Half-KFN with permutation test

² Half-KFN with bootstrap hypothesis test

TABLE IV
 DRIFT DETECTION RESULTS WITH REAL-WORLD DATASETS, MEAN OF p -VALUE AND STANDARD DEVIATION UNDER H_1 ($\delta = 0.05$). SEVEN ALGORITHMS ARE RUN 100 TIMES ON SOURCE AND TARGET SETS OF 500 SAMPLES EACH, GENERATED WITH DIFFERENT RANDOM SEEDS.

dataset	shift type	MMD	Energy	FR	KNN	SmoothKNN	Ours ¹	Ours ²
MNIST	adv	0.33 ± 0.26	0.38 ± 0.29	0.31 ± 0.25	0.35 ± 0.26	0.35 ± 0.26	0.02 ± 0.05	0.00 ± 0.00
	gn	0.46 ± 0.27	0.43 ± 0.27	0.45 ± 0.27	0.44 ± 0.28	0.44 ± 0.28	0.15 ± 0.18	0.02 ± 0.04
	img	0.24 ± 0.21	0.30 ± 0.25	0.20 ± 0.20	0.33 ± 0.27	0.33 ± 0.27	0.01 ± 0.03	0.00 ± 0.00
Fashion-MNIST	adv	0.27 ± 0.31	0.45 ± 0.31	0.27 ± 0.30	0.44 ± 0.31	0.43 ± 0.31	0.10 ± 0.13	0.00 ± 0.00
	gn	0.46 ± 0.29	0.51 ± 0.28	0.47 ± 0.29	0.52 ± 0.27	0.51 ± 0.27	0.25 ± 0.22	0.16 ± 0.22
	img	0.37 ± 0.25	0.46 ± 0.29	0.36 ± 0.25	0.45 ± 0.27	0.44 ± 0.27	0.13 ± 0.17	0.05 ± 0.10
CIFAR10	adv	0.52 ± 0.27	0.50 ± 0.30	0.53 ± 0.26	0.51 ± 0.30	0.50 ± 0.30	0.40 ± 0.31	0.00 ± 0.00
	gn	0.50 ± 0.27	0.50 ± 0.29	0.49 ± 0.27	0.48 ± 0.29	0.47 ± 0.29	0.40 ± 0.28	0.32 ± 0.32
	img	0.45 ± 0.29	0.50 ± 0.27	0.45 ± 0.29	0.50 ± 0.30	0.49 ± 0.30	0.39 ± 0.29	0.39 ± 0.31
Avg		0.40	0.45	0.39	0.45	0.44	0.21	0.10

¹ Half-KFN with permutation test

² Half-KFN with bootstrap hypothesis test

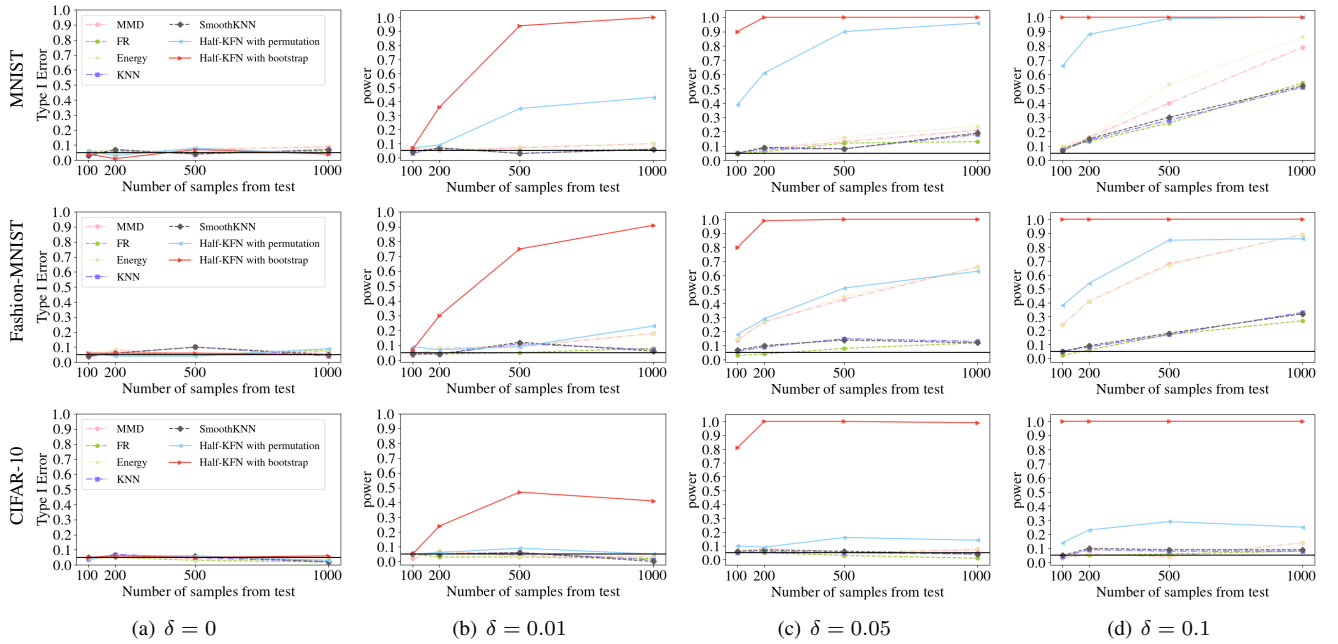


Fig. 6. Drift test on MNIST, Fashion-MNIST and CIFAR10 datasets with adversarial drift with parameter δ . (a) Figure demonstrates that the Type-I error rates of both two datasets are near significant level $\alpha = 0.05$, indicating effective control of Type-I errors. (b-d) Figures illustrate that with increasing sample size, the detection power of various two sample tests improves.

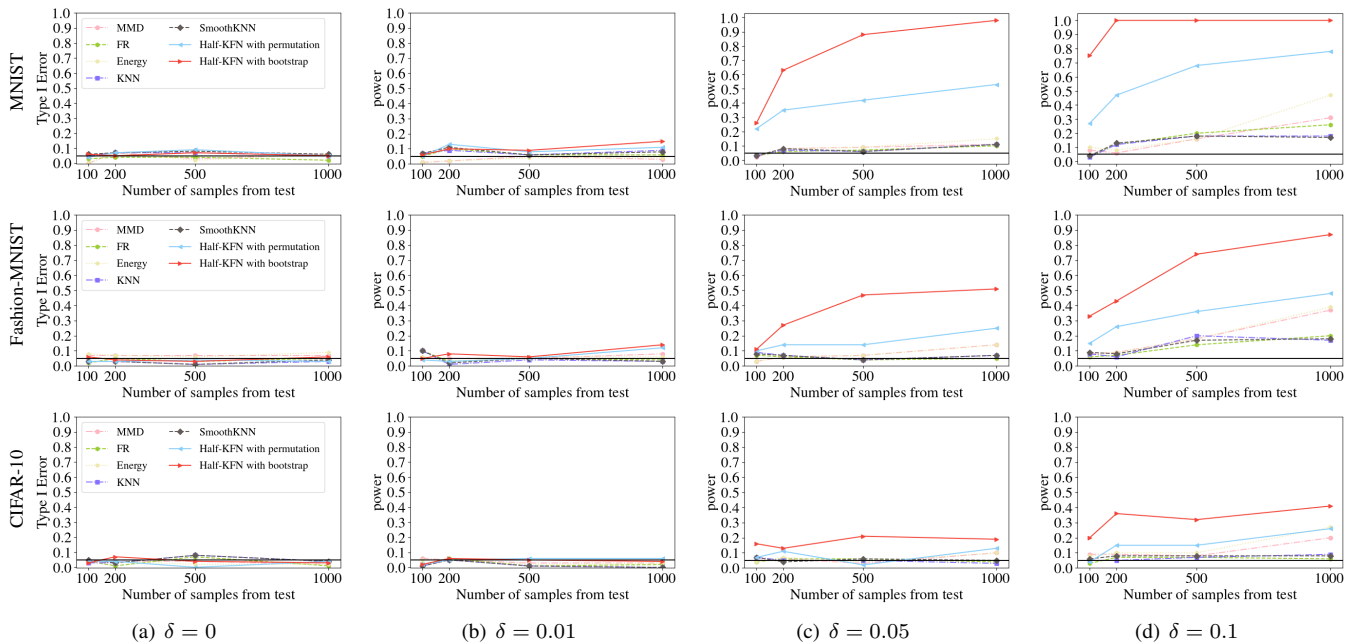


Fig. 7. Add Gaussian noise with a standard deviation of 100 to the samples with a proportion of δ in the MNIST, Fashion-MNIST and CIFAR10 test datasets. The experimental setup and explanation are similar to Fig. 6.

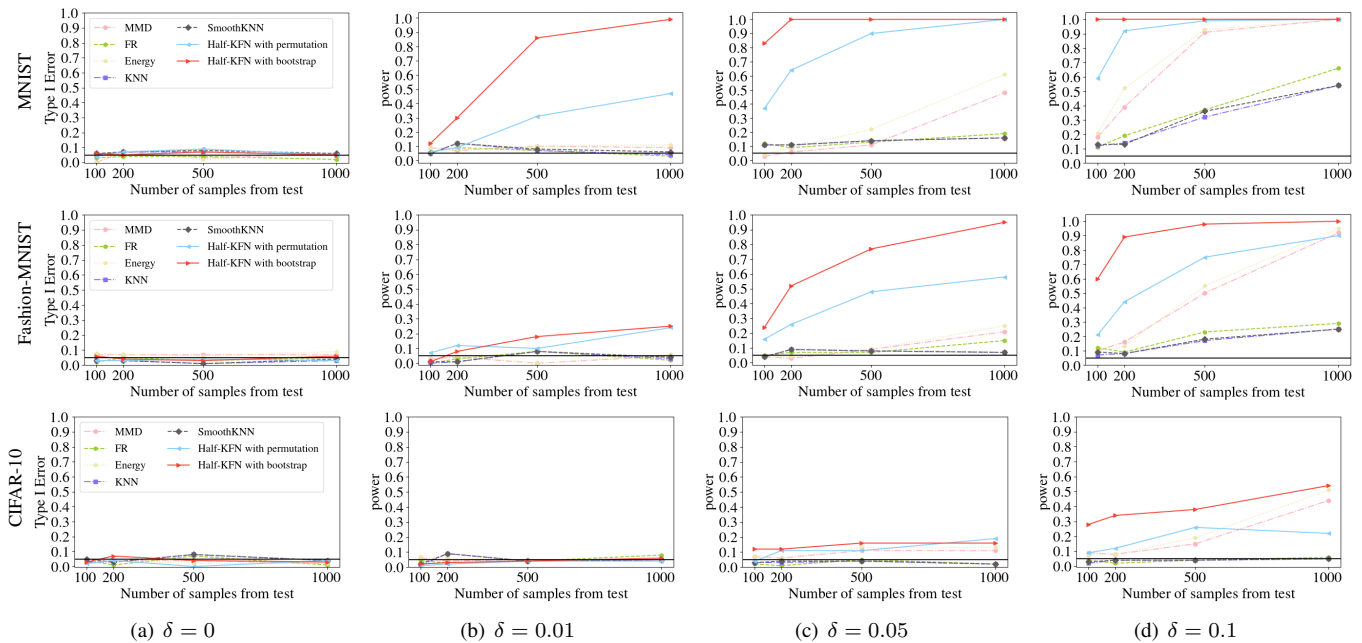


Fig. 8. Drift test on MNIST, Fashion-MNIST and CIFAR10 datasets with image drift with parameter δ . Image drift refers to the systematic augmentation of a subset of images in the test set, with a proportion of δ , using image generators. The experimental setup are similar to Fig. 6.

V. CONCLUSION AND DISCUSSION

A. Conclusion

In supervised learning, failure to promptly and accurately detect subtle covariate drift may cause a decline in model performance. To address the issue of small proportions of drift samples, this paper introduces a novel and efficient method called Half-KFN. In addition, we calculate the expectation and asymptotic variance of Half-KFN statistic, and we propose

using bootstrap to construct critical values for conducting hypothesis testing.

The following findings are observed:

1) Compared to traditional methods, the Half-KFN method exhibits a higher power, thereby demonstrating its reliability in detecting covariate drifts

2) Heightened sensitivity in detecting small proportions of covariance shift is exhibited by the Half-KFN, utilizing both

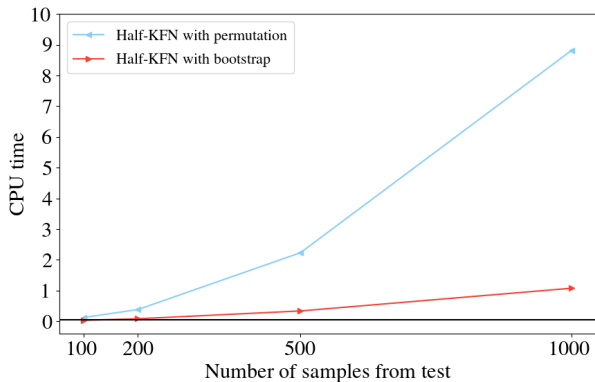


Fig. 9. Comparison of inference time for a single run between permutation test and bootstrap hypothesis test of Half-KFN on CPU. The x -axis denotes the sample size, and the y -axis represents the inference time.

permutation test and bootstrap hypothesis test, particularly in settings with smaller sample sizes. Conversely, when dealing with larger sample sizes, the bootstrap hypothesis test of the Half-KFN proves to be not only more precise but also quicker than permutation test for detecting even the subtle covariance drifts.

3) Experiments are conducted with different types and magnitudes of drift using simulated and real-world datasets, such as MNIST, Fashion-MNIST and CIFAR10. The stability of the Half-KFN is reflected in its ability to effectively control the Type-I error under the null hypothesis, thus ensuring reliable detection.

B. Discussion

Despite the constraints imposed by the limited scope of this paper, we have not been able to exhaustively present the specific scenarios where n_1 and n_2 are unequal in our experimental results. Nevertheless, based on the theorem elaborated in this paper, it is anticipated that under such conditions, the outcomes should still align with and confirm the conclusions drawn by the theorem. As the number of distant neighbors (k) and bootstrap iterations (M) increase, the principles and framework presented in this paper enable a more efficient detection of covariate drift. However, this enhancement comes at the cost of a notable surge in computational complexity. Furthermore, when dealing with higher data dimensions (L), the detection process becomes more intricate, posing additional challenges. Consequently, due to space limitations, an in-depth investigation and detailed analysis of these scenarios will be undertaken in future research endeavors.

APPENDIX A PROOF OF PROPOSITION 1

Proof. For all $t \in \{1, \dots, P\}$, define $T = T_{k, n_1} + \epsilon$ and $T^{(t)} = T_{k, n_1}^{(t)} + \epsilon_t$, where ϵ and ϵ_t 's are i.i.d from $N(0, \sigma^2)$.

Recall that

$$p = \frac{\sum_{t=1}^P (I(T \leq T^{(t)}))}{P}. \quad (\text{A.1})$$

If $p \cdot P = a$ means there are a values of t that no less than T . If H_0 in Section III-A holds and the permutations are drawn uniformly from the set of all permutations of $\{1, \dots, P\}$, then $T, T^{(1)}, \dots, T^{(P)}$ are exchangeable. Because we add ϵ_t 's in $T^{(t)}$'s, we can guarantee that all $T^{(t)}$'s are different with probability 1. Consequently, $U_P = p \cdot P$ is uniformly distributed in $\{1, \dots, P\}$. Thus,

$$\mathbb{P}(p \leq \alpha) = \mathbb{P}(p \cdot P \leq \alpha \cdot P) \quad (\text{A.2})$$

$$= \mathbb{P}(U_P \leq \lfloor \alpha \cdot P \rfloor) \quad (\text{A.3})$$

$$= \frac{\lfloor \alpha \cdot P \rfloor}{P} \quad (\text{A.4})$$

$$\leq \frac{\alpha \cdot P}{P} \quad (\text{A.5})$$

$$= \alpha \quad (\text{A.6})$$

where $\lfloor \cdot \rfloor$ is the floor function. \square

APPENDIX B PROOF OF THEOREM III.1

Proof. Since both Equation III.5 and Equation III.11 involve summation over i from 1 to n_1 , we only need to prove:

$$\sum_{j=n_1+1}^n I(A_{ij}^{(k)}) = \sum_{r=1}^k I_i(r) \quad (\text{B.1})$$

For $i \in \{1, \dots, n_1\}$, so $\hat{Y}_i \in p$, then

$$\begin{aligned} & \sum_{j=n_1+1}^n I(A_{ij}^{(k)}) \\ &= \sum_{j=n_1+1}^n I(\{\hat{Y}_j \text{ is one of the intra-class } k \text{ farthest neighbors of } \hat{Y}_i\}) \\ &= \sum_{j=1}^n I(\{\hat{Y}_j \in q \text{ is one of the intra-class } k \text{ farthest neighbors of } \hat{Y}_i\}) \\ &= \sum_{j=1}^n \sum_{r=1}^k I(\{\hat{Y}_j \in q \text{ is the } r\text{-th intra-class farthest neighbor of } \hat{Y}_i\}) \\ &= \sum_{r=1}^k \sum_{j=1}^n I(\{\hat{Y}_j \in q \text{ is the } r\text{-th intra-class farthest neighbor of } \hat{Y}_i\}) \\ &= \sum_{r=1}^k I(\{\text{find the } r\text{-th intra-class farthest neighbor of } \hat{Y}_i, \text{ and it belongs to } q\}) \\ &= \sum_{r=1}^k I(\{FN_i(r) \in q\}) \\ &= \sum_{r=1}^k I_i(r) \end{aligned} \quad (\text{B.2})$$

APPENDIX C PROOF OF THEOREM III.2

Proof. For $r = 1, 2, \dots, k$ and $i = 1, 2, \dots, n$, let the r -th intra-class farthest neighbor of \hat{Y}_i be denoted by $FN_i(r)$. Now, for $i \neq j$, let us consider the following five mutually exclusive and exhaustive probabilities:

$$\begin{aligned} p_1(r, s) &= P_{H_0}(FN_i(r) = \hat{Y}_j, FN_j(s) = \hat{Y}_i) \\ p_2(r, s) &= P_{H_0}(FN_i(r) = FN_j(s)) \\ p_3(r, s) &= P_{H_0}(FN_i(r) = \hat{Y}_j, FN_j(r) \neq \hat{Y}_i) \\ p_4(r, s) &= P_{H_0}(FN_i(r) \neq \hat{Y}_j, FN_j(r) = \hat{Y}_i) \end{aligned}$$

$p_5(r, s) = P_{H_0}(FN_i(r) \neq \hat{Y}_j, FN_j(r) \neq \hat{Y}_i, FN_i(r) \neq FN_j(s))$

Now, using

$$p_1(r, s) = \frac{1}{n-1} P_{H_0}(FN_i(r) = \hat{Y}_j | FN_j(s) = \hat{Y}_i)$$

we easily obtain $p_3(r, s) = p_4(r, s) = \frac{1}{n-1} - p_1(r, s)$ and $p_5(r, s) = \frac{n-3}{n-1} + p_1(r, s) - p_2(r, s)$

Define $I_i(r)$ as the indicator variable that takes the value 1 if \hat{Y}_i and its r -th farthest neighbor belong to the different sample. Now,

$$T_{k, n_1} = \frac{1}{n_1 k} \sum_{i=1}^{n_1} \sum_{r=1}^k I_i(r) \quad (\text{C.1})$$

$$E_{H_0}(T_{k, n_1}) = \frac{1}{n_1 k} n_1 k \frac{n_2}{n-1} = \frac{n_2}{n-1} \quad (\text{C.2})$$

$Var_{H_0}(T_{k, n_1})$

$$\begin{aligned} &= \frac{1}{n_1^2 k^2} Var_{H_0} \left(\sum_{i=1}^{n_1} \sum_{r=1}^k I_i(r) \right) \\ &= \frac{1}{n_1^2 k^2} \left(E_{H_0} \left(\sum_{i=1}^{n_1} \sum_{r=1}^k I_i(r) \right)^2 - \left(E_{H_0} \left(\sum_{i=1}^{n_1} \sum_{r=1}^k I_i(r) \right) \right)^2 \right) \\ &= \frac{1}{n_1^2 k^2} \left(\sum_{i=1}^{n_1} \sum_{j=1}^{n_1} \sum_{r=1}^k \sum_{s=1}^k P(I_i(r) = I_j(s) = 1) \right) - \left(\frac{n_2}{n-1} \right)^2 \\ &= \frac{1}{n_1^2 k^2} \left(\sum_{i=1}^{n_1} \sum_{r=1}^k P_{H_0}(I_i(r) = 1) \right) \\ &+ \frac{1}{n_1^2 k^2} \left(\sum_{i=1}^{n_1} \sum_{r=1}^k \sum_{s=1, s \neq r}^k P(I_i(r) = I_i(s) = 1) \right) \\ &+ \frac{1}{n_1^2 k^2} \left(\sum_{i=1}^{n_1} \sum_{j=1, j \neq i}^{n_1} \sum_{r=1}^k \sum_{s=1}^k P(I_i(r) = I_j(s) = 1) \right) \\ &- \left(\frac{n_2}{n-1} \right)^2 \end{aligned} \quad (\text{C.3})$$

Note that

$$\sum_{i=1}^{n_1} \sum_{r=1}^k P_{H_0}(I_i(r) = 1) = \frac{kn_1 n_2}{n-1} \quad (\text{C.4})$$

$$\begin{aligned} &\sum_{i=1}^{n_1} \sum_{r=1}^k \sum_{s=1, s \neq r}^k P(I_i(r) = I_i(s) = 1) \\ &= n_1 k(k-1) \frac{n_2(n_2-1)}{(n-1)(n-2)} \end{aligned} \quad (\text{C.5})$$

$$\begin{aligned} &\sum_{i=1}^{n_1} \sum_{j=1, j \neq i}^{n_1} \sum_{r=1}^k \sum_{s=1}^k P(I_i(r) = I_j(s) = 1) \\ &= n_1(n_1-1) \sum_{r=1}^k \sum_{s=1}^k \beta(r, s) \end{aligned} \quad (\text{C.6})$$

where

$$\beta(r, s) = \frac{n_2}{n-2} p_2(r, s) + \frac{n_2(n_2-1)}{(n-1)(n-2)} p_5(r, s) \quad (\text{C.7})$$

$Var_{H_0}(T_{k, n_1})$ can be simplified to the expression:

$$\begin{aligned} &Var_{H_0}(T_{k, n_1}) \\ &= \frac{n_2(n_2-1)(n_1-1)}{n_1(n-1)(n-2)} \frac{\sum_{r=1}^k \sum_{s=1}^k p_1(r, s)}{k^2} \\ &+ \frac{n_2(n_1-1)}{(n-1)(n-2)} \frac{\sum_{r=1}^k \sum_{s=1}^k p_2(r, s)}{k^2} \\ &+ \frac{n_2(nn_1 - n - n_1 - kn_1(n+n_2) + k(3n_1 + 2n_2 - 2) + 1)}{kn_1(n-1)^2(n-2)} \end{aligned} \quad (\text{C.8})$$

Bootstrap is performed in populations p and q , assuming M resampling operations, with each operation maintaining a consistent sample size. This process generates M sets of random samples, with each set undergoing the aforementioned calculation process to obtain the statistic $T_{k, n_1, m}$, where $m = 1, \dots, M$. Subsequently, the average of these M statistics

is computed as $\overline{T_{k, n_1}} = \frac{\sum_{m=1}^M T_{k, n_1, m}}{M}$.

According to the Central Limit Theorem, when the sample size is sufficiently large, regardless of the distribution of the population, $\overline{T_{k, n_1}}$ follows a normal distribution. Thus,

$$\mu = \lim_{n \rightarrow \infty} E_{H_0}(T_{k, n_1, m}) = \lim_{n \rightarrow \infty} \frac{n_2}{n-1} = \lambda_2 \quad (\text{C.9})$$

$$\begin{aligned} \sigma^2 &= \lim_{n \rightarrow \infty} Var_{H_0}(T_{k, n_1, m}) \\ &= \lambda_2^2 \frac{\sum_{r=1}^k \sum_{s=1}^k p_1(r, s)}{k^2} \\ &+ \lambda_1 \lambda_2 \frac{\sum_{r=1}^k \sum_{s=1}^k p_2(r, s)}{k^2} \end{aligned} \quad (\text{C.10})$$

□

REFERENCES

- [1] V. Nasteski, "An overview of the supervised machine learning methods," *Horizons. b*, vol. 4, no. 51-62, p. 56, 2017.
- [2] J. E. Van Engelen and H. H. Hoos, "A survey on semi-supervised learning," *Machine learning*, vol. 109, no. 2, pp. 373-440, 2020.
- [3] Z.-H. Zhou, "A brief introduction to weakly supervised learning," *National Science Review*, vol. 5, no. 1, pp. 44-53, 2018.
- [4] J. G. Moreno-Torres, T. Raeder, R. Alaiz-Rodríguez, N. V. Chawla, and F. Herrera, "A unifying view on dataset shift in classification," *Pattern recognition*, vol. 45, no. 1, pp. 521-530, 2012.
- [5] F. M. Polo, R. Izbicki, E. G. Lacerda Jr, J. P. Ibieta-Jimenez, and R. Vicente, "A unified framework for dataset shift diagnostics," *Information Sciences*, vol. 649, p. 119612, 2023.
- [6] O. Cobb and A. Van Looveren, "Context-aware drift detection," in *International conference on machine learning*. PMLR, 2022, pp. 4087-4111.
- [7] A. Liu, J. Lu, and G. Zhang, "Concept drift detection via equal intensity k-means space partitioning," *IEEE transactions on cybernetics*, vol. 51, no. 6, pp. 3198-3211, 2020.
- [8] X. Wang, Q. Kang, M. Zhou, L. Pan, and A. Abusorrah, "Multiscale drift detection test to enable fast learning in nonstationary environments," *IEEE Transactions on Cybernetics*, vol. 51, no. 7, pp. 3483-3495, 2020.

- [9] H. Shimodaira, "Improving predictive inference under covariate shift by weighting the log-likelihood function," *Journal of statistical planning and inference*, vol. 90, no. 2, pp. 227–244, 2000.
- [10] M. Awais, M. T. B. Iqbal, and S.-H. Bae, "Revisiting internal covariate shift for batch normalization," *IEEE Transactions on Neural Networks and Learning Systems*, vol. 32, no. 11, pp. 5082–5092, 2020.
- [11] G. Wilson and D. J. Cook, "A survey of unsupervised deep domain adaptation," *ACM Transactions on Intelligent Systems and Technology (TIST)*, vol. 11, no. 5, pp. 1–46, 2020.
- [12] I. J. Goodfellow, J. Shlens, and C. Szegedy, "Explaining and harnessing adversarial examples," in *3rd International Conference on Learning Representations, ICLR 2015*, Y. Bengio and Y. LeCun, Eds., 2015. [Online]. Available: <http://arxiv.org/abs/1412.6572>
- [13] H. Raza, H. Cecotti, Y. Li, and G. Prasad, "Adaptive learning with covariate shift-detection for motor imagery-based brain-computer interface," *Soft Computing*, vol. 20, pp. 3085–3096, 2016.
- [14] H. Raza, G. Prasad, and Y. Li, "Adaptive learning with covariate shift-detection for non-stationary environments," in *2014 14th UK Workshop on Computational Intelligence (UKCI)*. IEEE, 2014, pp. 1–8.
- [15] S. Rabanser, S. Günnemann, and Z. C. Lipton, "Failing loudly: An empirical study of methods for detecting dataset shift," in *Proceedings of the 33rd International Conference on Neural Information Processing Systems*, 1396–1408, 2019.
- [16] J. C. Sisniega, V. Rodríguez, G. Moltó, and Á. L. García, "Efficient and scalable covariate drift detection in machine learning systems with serverless computing," *Future Generation Computer Systems*, vol. 161, pp. 174–188, 2024.
- [17] Y. Xu and D. Klabjan, "Concept drift and covariate shift detection ensemble with lagged labels," in *2021 IEEE International Conference on Big Data (Big Data)*. IEEE, 2021, pp. 1504–1513.
- [18] F. Maia Polo and R. Vicente, "Effective sample size, dimensionality, and generalization in covariate shift adaptation," *Neural Computing and Applications*, vol. 35, no. 25, pp. 18 187–18 199, 2023.
- [19] A. Kore, E. Abbasi Bavil, V. Subasri, M. Abdalla, B. Fine, E. Dolatabadi, and M. Abdalla, "Empirical data drift detection experiments on real-world medical imaging data," *Nature Communications*, vol. 15, no. 1, p. 1887, 2024.
- [20] A. Podkopaev and A. Ramdas, "Tracking the risk of a deployed model and detecting harmful distribution shifts," *Tenth International Conference on Learning Representations*, 2022. [Online]. Available: <https://par.nsf.gov/biblio/10334960>
- [21] A. Chan, A. Alaa, Z. Qian, and M. Van Der Schaar, "Unlabelled data improves bayesian uncertainty calibration under covariate shift," in *International conference on machine learning*. PMLR, 2020, pp. 1392–1402.
- [22] S. Park, O. Bastani, J. Weimer, and I. Lee, "Calibrated prediction with covariate shift via unsupervised domain adaptation," in *International Conference on Artificial Intelligence and Statistics*. PMLR, 2020, pp. 3219–3229.
- [23] F. You, J. Li, and Z. Zhao, "Test-time batch statistics calibration for covariate shift," *CoRR*, vol. abs/2110.04065, 2021. [Online]. Available: <https://arxiv.org/abs/2110.04065>
- [24] S. Castle, R. Schwarzenberg, and M. Pourvali, "Detecting covariate drift with explanations," in *CCF International Conference on Natural Language Processing and Chinese Computing*. Springer, 2021, pp. 317–322.
- [25] Z. Lipton, Y.-X. Wang, and A. Smola, "Detecting and correcting for label shift with black box predictors," in *International Conference on Machine Learning*. PMLR, 3122–3130, 2018.
- [26] M. A. Wijaya, D. Kazhdan, B. Dimanov, and M. Jamnik, "Failing conceptually: Concept-based explanations of dataset shift," *arXiv preprint arXiv:2104.08952*, 2021.
- [27] D. S. Mukherjee, D. Bhandari, and N. G. Yeri, "Detecting distributional shift responsible for predictive model's failure," in *2022 International Conference for Advancement in Technology (ICONAT)*. IEEE, 2022, pp. 1–5.
- [28] F. Biggs, A. Schrab, and A. Gretton, "Mmd-fuse: Learning and combining kernels for two-sample testing without data splitting," *Advances in Neural Information Processing Systems*, vol. 36, 2024.
- [29] A. Gretton, K. M. Borgwardt, M. J. Rasch, B. Schölkopf, and A. Smola, "A kernel two-sample test," *The Journal of Machine Learning Research*, vol. 13, no. 1, pp. 723–773, 2012.
- [30] A. Schrab, I. Kim, M. Albert, B. Laurent, B. Guedj, and A. Gretton, "Mmd aggregated two-sample test," *Journal of Machine Learning Research*, vol. 24, no. 194, pp. 1–81, 2023.
- [31] J. H. Friedman and L. C. Rafsky, "Multivariate generalizations of the wald-wolfowitz and smirnov two-sample tests," *The Annals of Statistics*, 697–717, 1979.
- [32] C. Hsiao, M. Liu, R. Stanton, M. McGee, Y. Qian, and R. H. Scheuermann, "Mapping cell populations in flow cytometry data for cross-sample comparison using the friedman-rafsky test statistic as a distance measure," *Cytometry Part A*, vol. 89, no. 1, pp. 71–88, 2016.
- [33] B. Aslan and G. Zech, "Statistical energy as a tool for binning-free, multivariate goodness-of-fit tests, two-sample comparison and unfolding," *Nuclear Instruments and Methods in Physics Research Section A: Accelerators, Spectrometers, Detectors and Associated Equipment*, vol. 537, no. 3, pp. 626–636, 2005.
- [34] G. Zech, "Scaling property of the statistical two-sample energy test," *arXiv preprint arXiv:1804.10599*, 2018.
- [35] M. F. Schilling, "Multivariate two-sample tests based on nearest neighbors," *Journal of the American Statistical Association*, vol. 81, no. 395, pp. 799–806, 1986.
- [36] N. Henze, "A multivariate two-sample test based on the number of nearest neighbor type coincidences," *The Annals of Statistics*, vol. 16, no. 5, pp. 772–783, 1988.
- [37] J. Djolonga and A. Krause, "Learning implicit generative models using differentiable graph tests," *Stat*, vol. 1050, p. 4, 2017.
- [38] P. K. Mondal, M. Biswas, and A. K. Ghosh, "On high dimensional two-sample tests based on nearest neighbors," *Journal of Multivariate Analysis*, vol. 141, pp. 168–178, 2015.
- [39] M. F. Schilling, "Mutual and shared neighbor probabilities: finite-and infinite-dimensional results," *Advances in Applied Probability*, vol. 18, no. 2, pp. 388–405, 1986.
- [40] L. M. Chihara and T. C. Hesterberg, *Mathematical statistics with resampling and R*. John Wiley & Sons, 2022.
- [41] R. H. Lock, P. F. Lock, K. L. Morgan, E. F. Lock, and D. F. Lock, *Statistics: Unlocking the power of data*. John Wiley & Sons, 2020.
- [42] C. DiCiccio, S. Vasudevan, K. Basu, K. Kenthapadi, and D. Agarwal, "Evaluating fairness using permutation tests," in *Proceedings of the 26th ACM SIGKDD International Conference on Knowledge Discovery & Data Mining*, 2020, pp. 1467–1477.
- [43] P. Good, *Permutation tests: a practical guide to resampling methods for testing hypotheses*. Springer Science & Business Media, 2013.
- [44] B. J. LaFleur and R. A. Greevy, "Introduction to permutation and resampling-based hypothesis tests," *Journal of Clinical Child & Adolescent Psychology*, vol. 38, no. 2, pp. 286–294, 2009.
- [45] J. Frossard and O. Renaud, "Permutation tests for regression, anova, and comparison of signals: the permuco package," *Journal of Statistical Software*, vol. 99, pp. 1–32, 2021.
- [46] H. Yu and A. D. Hutson, "A robust spearman correlation coefficient permutation test," *Communications in Statistics-Theory and Methods*, vol. 53, no. 6, pp. 2141–2153, 2024.
- [47] S. Shekhar, I. Kim, and A. Ramdas, "A permutation-free kernel independence test," *Journal of Machine Learning Research*, vol. 24, no. 369, pp. 1–68, 2023.
- [48] T. C. Hesterberg, "What teachers should know about the bootstrap: Resampling in the undergraduate statistics curriculum," *The american statistician*, vol. 69, no. 4, pp. 371–386, 2015.
- [49] U. Yolcu, E. Egrioglu, E. Bas, O. C. Yolcu, and A. Z. Dalar, "Probabilistic forecasting, linearity and nonlinearity hypothesis tests with bootstrapped linear and nonlinear artificial neural network," *Journal of Experimental & Theoretical Artificial Intelligence*, vol. 33, no. 3, pp. 383–404, 2021.
- [50] M. R. Chernick and R. A. LaBudde, *An introduction to bootstrap methods with applications to R*. John Wiley & Sons, 2014.
- [51] A. K. Dwivedi, I. Mallawaarachchi, and L. A. Alvarado, "Analysis of small sample size studies using nonparametric bootstrap test with pooled resampling method," *Statistics in medicine*, vol. 36, no. 14, pp. 2187–2205, 2017.
- [52] E. L. Lehmann, J. P. Romano, and G. Casella, *Testing statistical hypotheses*. Springer Science & Business Media, 2006.
- [53] J. Rauber, R. Zimmermann, M. Bethge, and W. Brendel, "Foolbox native: Fast adversarial attacks to benchmark the robustness of machine learning models in pytorch, tensorflow, and jax," *Journal of Open Source Software*, vol. 5, no. 53, p. 2607, 2020.
- [54] J. Rauber, W. Brendel, and M. Bethge, "Foolbox: A python toolbox to benchmark the robustness of machine learning models," in *Reliable Machine Learning in the Wild Workshop, 34th International Conference on Machine Learning*, 2017. [Online]. Available: <http://arxiv.org/abs/1707.04131>